Supporting information

The effect of nanoscaffold porosity and surface chemistry on the Li-ion conductivity of $LiBH_4$-$LiNH_2$/metal oxide nanocomposites

Laura M. de Kort, Justine Harmel, Petra de Jongh, Peter Ngene*

Inorganic Chemistry and Catalysis, Debye Institute for Nanomaterials Science, Utrecht University, Universiteitsweg 99, 3584 DX Utrecht, Netherlands

* Corresponding author: P.Ngene@uu.nl

S1. Synthesis procedure of mesoporous oxides

Mesoporous silica (MCM-41 and SBA-15) and aluminated silica (Al-SBA-15) were synthesized following the procedures described here.

MCM-41 was synthesized based on the procedure of Cheng et al.[52] In general, 40.9 g hexadecyltrimethylammonium bromide (CTAB, > 96.0%, Aldrich) and 28.8 g tetramethylammonium hydroxide (TMAOH, 25 wt% in H_2O, Aldrich) was dissolved in 297.7 g deionized water. While stirring at 30 °C, 25.0 g SiO_2 (AEROSIL 380, Evonik) was added and allowed to react for 120 minutes. After 120 minutes, stirring was stopped and the mixture was aged at 30 °C for 24 hours. The obtained mixture was transferred to a Teflon-lined stainless-steel autoclave and placed in an oven preheated at 140 °C to react further for 40 hours. After synthesis, the product was filtrated and washed with deionized water to remove all surfactants. Finally, the product was dried at 120 °C in static air for 8 hours and calcined at 550 °C (heating rate 1.5 °C min^{-1}) for 12 hours.

SBA-15 was synthesized following the procedure by Lee et al.[53] Typically, 23.4 g Pluronic P123 ($EO_{20}PO_{70}EO_{20}$, average Mw = 5800, Aldrich) was dissolved in 606.8 g of deionized water and 146.4 hydrochloric acid. To achieve thermal equilibrium, the mixture was stirred vigorously for at least three hours at 55 °C. Then, 50.0 g of tetraethyl orthosilicate (TEOS, > 99%) was added at once, after which the mixture was stirred for two minutes at 600 rpm. After 2 minutes, the stirring bar was removed, and the reaction bottle was closed. The mixture was kept at 55 °C for 24 hours. Following, the SBA-15 was allowed to condensate further for 24 hours at 45, 60, 75, 90, 100 or 120 °C. With this final condensation step the pore structure can be controlled. The as-prepared SBA-15 was filtered and washed with deionized water using a Büchner funnel until no HCl was left in the solution. The material was dried at 60 °C for 3 days and calcined in static air at 550 °C (heating rate 1 °C min^{-1}) for 6 hours.

Aluminated SBA-15 was prepared following the procedure by Baca et al.[54] A solution of aluminium isopropoxide in anhydrous isopropanol or cyclohexane was added to SBA-15 dried at 450 °C for 2 hours. This was left to react overnight at room temperature while stirring. The obtained suspension was washed with the corresponding anhydrous solvent before calcination at 500 °C for 4 hours. Depending on the amount of aluminium isopropoxide used, Al-SBA-15 with a Si/Al ratio of 20:1 or 10:1 were prepared, further referred to as Al(20)- and Al(10)-SBA-15.

S2. Comparison of nanocomposite conductivity to nanoconfined $LiBH_4$ and $LiNH_2$

The conductivity data for the $LiBH_4$-$LiNH_2$ mixtures, $LiBH_4$-$LiNH_2$/metal oxide nanocomposites and $LiBH_4$/metal oxide nanocomposites is based on Nyquist plots, as shown in Figure S1 and S2.

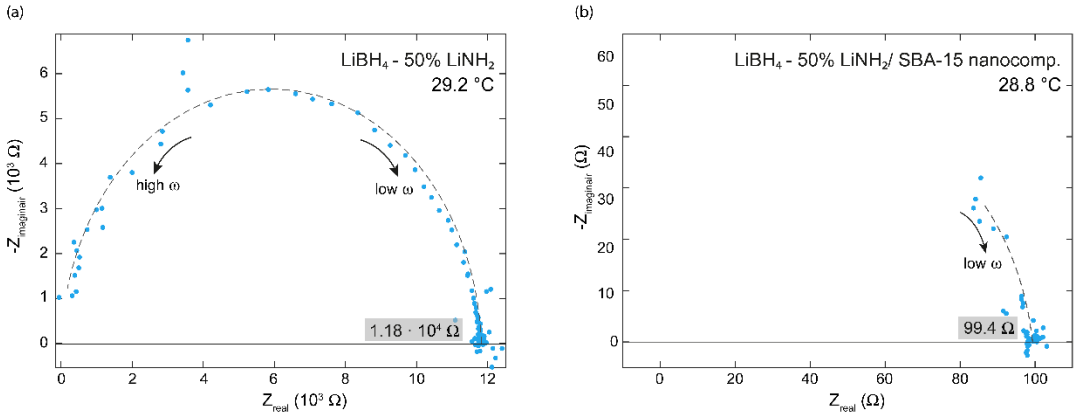

Figure S1 – Exemplary Nyquist plots for (a) non-confined and (b) confined $LiBH_4$ – 50% $LiNH_2$ obtained at 29 °C.

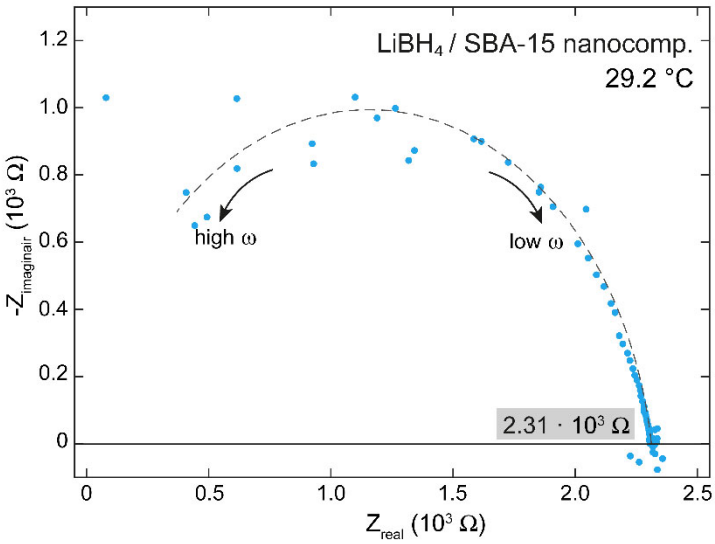

Figure S2 – Exemplary Nyquist plots for confined $LiBH_4$ obtained at 29 °C.

S2. Calculation for the synthesis of solid solutions and nanocomposites

For the preparation of (1-*x*)$LiBH_4$ - *x* $LiNH_2$ the mass ratio was calculated using the molecular weight of $LiBH_4$ (21.78 g mol^{-1}) and $LiNH_2$ (22.96 g mol^{-1}) and the intended molar fraction of the final product. Nanoconfined $LiBH_4$-$LiNH_2$ was synthesized via melt infiltration of solid solutions containing 30, 40 and 50 mol% $LiNH_2$ in a mesoporous oxide. The required amount of solid solution was calculated based on the specific pore volume of the oxide (from N_2 physisorption), the specific volume of $LiBH_4$ (0.66 g cm^{-3}) and the specific volume of $LiNH_2$ (1.18 g cm^{-3}). The compositions of the sample in weight percentage and molar percentage are given in Table S1.

Table S1 – Composition of solid solutions and nanocomposites in wt% and mol%

Pellets	**Weight percentage**			**Molar percentage**		
Solid solutions	**$LiBH_4$**	**$LiNH_2$**		**$LiBH_4$**	**$LiNH_2$**	
$LiBH_4$-5%$LiNH_2$	94%	6%		95%	5%	
$LiBH_4$-15%$LiNH_2$	84%	16%		85%	15%	
$LiBH_4$-30%$LiNH_2$	68%	32%		70%	30%	
$LiBH_4$-40%$LiNH_2$	59%	41%		60%	40%	
$LiBH_4$-50%$LiNH_2$	49%	51%		50%	50%	
$LiBH_4$-67%$LiNH_2$	32%	68%		33%	67%	
$LiBH_4$-75%$LiNH_2$	24%	76%		25%	75%	
Nanoconfined solid solutions	**$LiBH_4$**	**$LiNH_2$**	**Oxide**	**$LiBH_4$**	**$LiNH_2$**	**Oxide**
$LiBH_4$-30%$LiNH_2$/MCM-41	36%	17%	47%	52%	23%	25%
$LiBH_4$-40%$LiNH_2$/MCM-41	32%	22%	46%	46%	30%	24%
$LiBH_4$-50%$LiNH_2$/MCM-41	27%	28%	45%	38%	38%	24%
$LiBH_4$-50%$LiNH_2$/SBA-15_45C	18%	19%	62%	31%	31%	38%
$LiBH_4$-50%$LiNH_2$/SBA-15_60C	18%	19%	64%	30%	30%	39%
$LiBH_4$-50%$LiNH_2$/SBA-15_75C	22%	23%	55%	35%	34%	31%
$LiBH_4$-50%$LiNH_2$/SBA-15_90C	21%	23%	56%	34%	34%	32%
$LiBH_4$-50%$LiNH_2$/SBA-15_100C	26%	28%	46%	38%	38%	24%
$LiBH_4$-50%$LiNH_2$/SBA-15_120C	26%	27%	47%	38%	37%	25%
$LiBH_4$-50%$LiNH_2$/SBA_Si/Al_no_grafting	26%	27%	47%	37%	37%	25%
$LiBH_4$-50%$LiNH_2$/SBA_Si/Al_20	25%	26%	49%	37%	37%	26%
$LiBH_4$-50%$LiNH_2$/SBA_Si/Al_10	25%	26%	49%	37%	37%	25%
$LiBH_4$-50%$LiNH_2$/Al_2O_3	17%	18%	65%	31%	31%	39%

S3. XRD and DRIFTS data of $LiBH_4$-$LiNH_2$ solid solutions

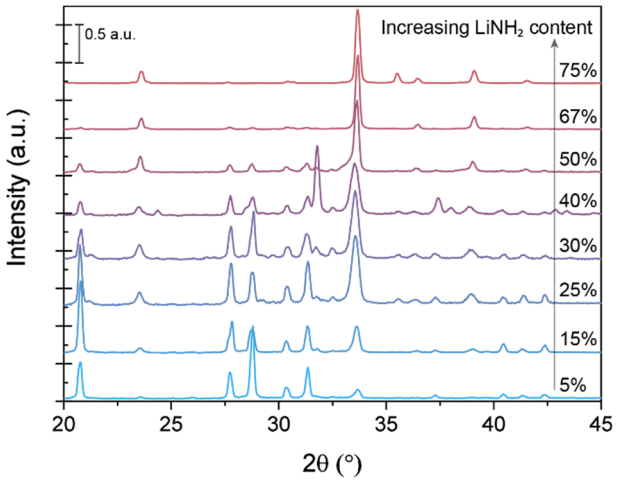

Figure S3 – XRD patterns of the (1-*x*)$LiBH_4$ – *x* $LiNH_2$ with different molar percentage of $LiNH_2$.

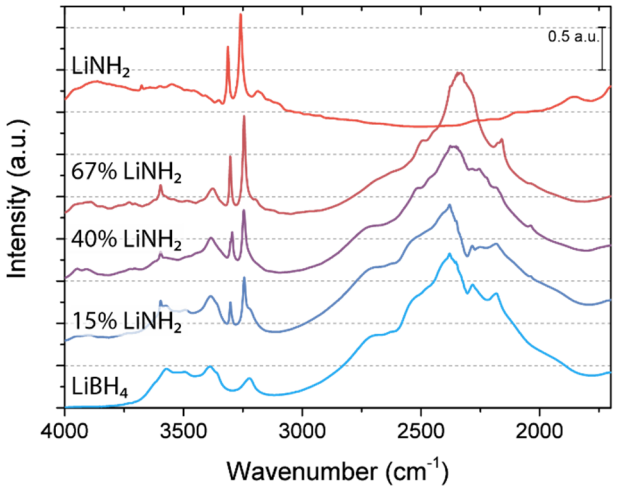

Figure S4 – DRIFTS spectra of $LiBH_4$-$LiNH_2$ solid solutions containing 15, 40 and 67 mol% $LiNH_2$. For comparison, the DRIFTS spectra of pure $LiBH_4$ and $LiNH_2$ are included.

S4. Confirmation of successful nanoconfinement

In Figure S2 (a) the XRD patterns of the $LiBH_4$ - 50% $LiNH_2$ solid solution and $LiBH_4$ - 50% $LiNH_2$/MCM-41 nanocomposite are shown. In Figure S2 (b) the N_2 physisorption isotherms of $LiBH_4$- 50% $LiNH_2$/MCM-41 with different degrees of pore filling are provided. Both techniques provide additional confirmation that the $LiBH_4$-$LiNH_2$ solid solution containing 50 mol% $LiNH_2$ is successfully confined in the pores of the mesoporous SiO_2 (MCM-41) scaffold.

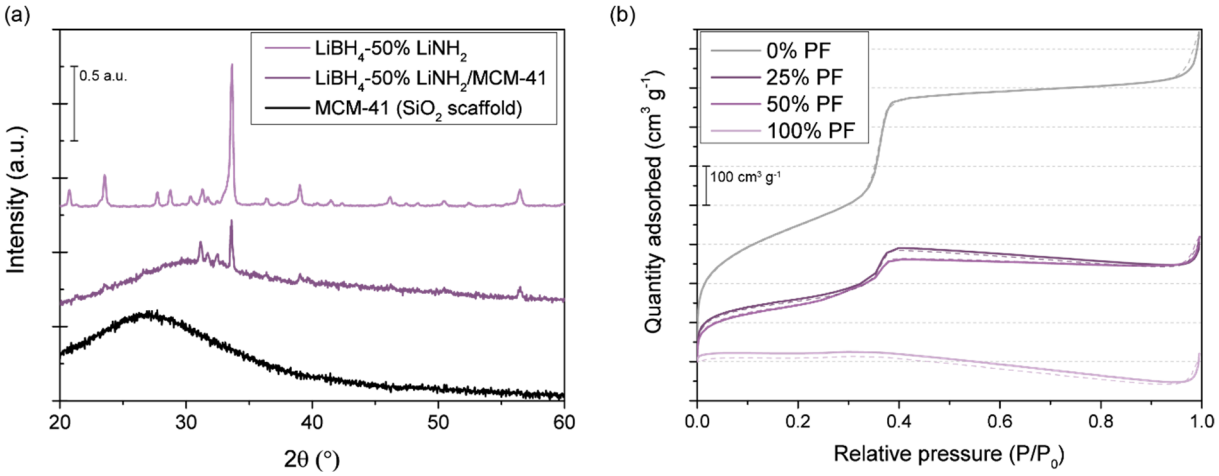

Figure S5 – (a) XRD patterns of $LiBH_4$ - 50% $LiNH_2$ and nanoconfined $LiBH_4$ – 50% $LiNH_2$. The XRD pattern of MCM-41 is shown for comparison. (b) N_2 physisorption isotherms of $LiBH_4$ - 50 % $LiNH_2$/MCM-41 nanocomposites with pore filling of 25, 50 and 100%.

S5. Comparison of nanocomposite conductivity to nanoconfined $LiBH_4$ and $LiNH_2$

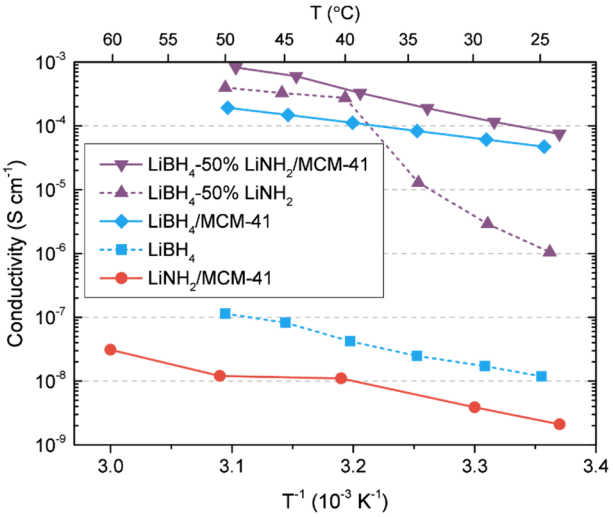

Figure S6 – Arrhenius plot illustrating the change in conductivity of $LiBH_4$, $LiNH_2$ and $LiBH_4$-$LiNH_2$ upon nanoconfinement in a mesoporous SiO_2 (MCM-41) scaffold.

S6. Nitrogen physisorption of mesoporous oxides

N_2 physisorption measurements were used to determine the porosity (pore volume, surface area and pore diameter) of the metal oxide scaffolds. The surface area and pore size distribution were determined with, respectively, a Brunauer-Emmett-Teller (BET) analysis and a Barrett-Joyner-Halenda analysis on the desorption branch of the isotherm.

Table S2 – Porosity of metal oxide scaffolds from N_2 physisorption

Scaffold	Synthesis parameter	Pore volume ($cm^3\ g^{-1}$)	BET Surface area ($m^2\ g^{-1}$)	Pore diameter (nm)
MCM-41				
	n.a.	1.11	1071.4	2.8
SBA-15	$T_{condensation}$			
	45 °C	0.54	609.9	5.1
	60 °C	0.51	610.5	6.3
	75 °C	0.74	834.1	7.4
	90 °C	0.71	720.9	7.9
	100 °C	1.06	805.1	8.3
	120 °C	1.00	628.7	6.9
Al-SBA-15	Si/Al			
	unmodified	0.99	726.3	6.6
	20	0.92	657.2	6.7
	10	0.92	643.4	6.6
γ-Al_2O_3				
	n.a.	0.48	188.3	9.3

S7. Conductivity correlation to pore diameter, surface area and pore volume

To be able to determine how $LiBH_4$-$LiNH_2$/metal oxide nanocomposite conductivity is influenced by the scaffold pore structure, the conductivity is correlated to the individual properties of the scaffold, e.g. pore volume, surface area and pore diameter. Additionally, the conductivity of LiBH4/metal oxide nanocomposites is correlated to scaffold pore volume.

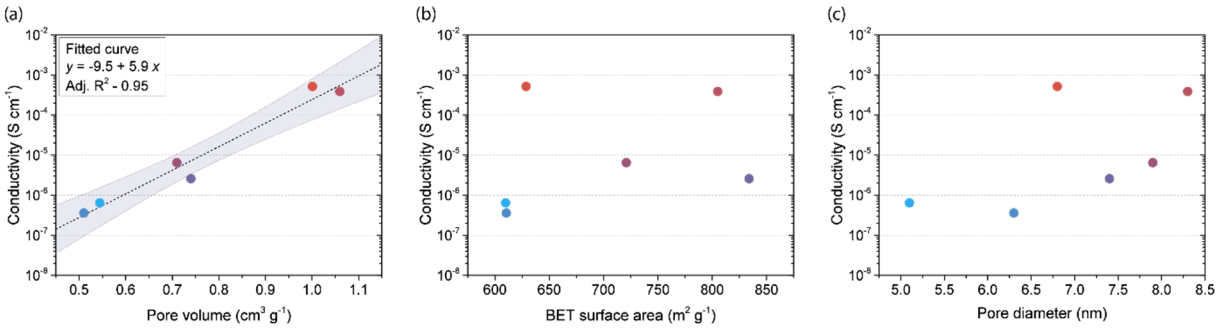

Figure S7 – Correlations between $LiBH_4$-$LiNH_2$/metal oxide nanocomposite conductivity and (a) pore volume, (b) BET surface area and (c) average pore diameter of the applied SBA-15 scaffold. A high correlation between conductivity and pore volume is found and shown with a linear fit and 95% confidence interval.

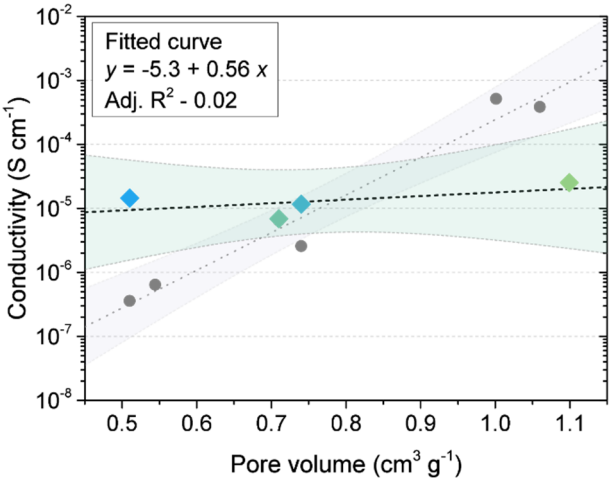

Figure S8 – Correlation between $LiBH_4$/metal oxide nanocomposite conductivity and pore volume based on SBA-15 scaffolds prepared with T_c = 60 °C (blue), 75 °C, 90 °C and 120 °C (green). For comparison, the correlation found for $LiBH_4$-$LiNH_2$/metal oxide nanocomposites (Figure S5a) is shown in grey, as well as the result for a similar analysis for nanoconfined LiBH4. Here, no correlation is found as can be seen by the low correlation coefficient.